

# Spectral and spatial variations of the diffuse $\gamma$ -ray background in the vicinity of the Galactic plane and possible nature of the feature at 130 GeV

Alexey Boyarsky<sup>a,b</sup>, Denys Malyshev<sup>b,\*</sup>, Oleg Ruchayskiy<sup>c</sup>

<sup>a</sup>Instituut-Lorentz for Theoretical Physics, Universiteit Leiden, Niels Bohrweg 2, Leiden, The Netherlands

<sup>b</sup>Bogolyubov Institute of Theoretical Physics, Kyiv, Ukraine

<sup>c</sup>CERN Physics Department, Theory Division, CH-1211 Geneva 23, Switzerland

## ARTICLE INFO

## ABSTRACT

We study the properties of the diffuse  $\gamma$ -ray background around the Galactic plane at energies 20–200 GeV. We find that the spectrum of this emission possesses significant spacial variations with respect to the average smooth component. The positions and shapes of these spectral features change with the direction on the sky. We therefore argue that the spectral feature around 130 GeV, found in several regions around the Galactic Center and in the Galactic plane in Bringmann et al. (2012) [1], Weniger (2012) [2], Tempel et al. (2012) [3], and Su and Finkbeiner (2012) [4], cannot be interpreted with confidence as a  $\gamma$ -ray line, but may be a component of the diffuse background and can be of instrumental or astrophysical origin. Therefore, the dark matter origin of this spectral feature becomes dubious.

© 2013 The Authors. Published by Elsevier B.V. Open access under [CC BY-NC-SA license](https://creativecommons.org/licenses/by-nc-sa/4.0/).

## 1. Introduction

It has been recently reported in [1] and further investigated in [2] and in [4]<sup>1</sup> that the  $\gamma$ -ray emission from the region around the Galactic Center (GC) exhibits a line-like excess at the energies  $\sim 130$  GeV. An interest to this result is based on the expectation that any signal of astrophysical origin at high energies would have a broad (compared to the Fermi spectral resolution) spectral shape. Diffuse emission with the line-like spectrum has therefore been considered as an exotic one, e.g. as a “smoking gun” for dark matter annihilation [5] (see e.g. [6,7] for review). In particular, “Higgs in space” scenario [8] predicts a  $\gamma$ -ray line at  $\sim 130$  GeV for the Higgs mass around 125 GeV as seen by the LHC [9,10].

The region of [1,2] was selected by maximizing signal-to-noise ratio for the expected dark matter annihilation signal. The preprints of [1,2] were followed by [3] where the claim was confirmed and it was demonstrated that a similar excess originates from several regions of the size  $\sim 3^\circ$  around the Galactic plane. A number of works [3,11–15] have discussed possible interpretations and origin of this spectral feature, see [7] for the review. The search for  $\gamma$ -ray lines,

based on the 2-year data, performed by the Fermi collaboration [16] did not reveal any lines but had not comment on the origin of the observed excess.

It was demonstrated in the first version of this paper (1205.4700v1) that spectral features with the significance, similar to that of the excess observed in the Galactic Center region around 130 GeV can be also found at other energies in different regions of the sky. It was then argued in [17,18]<sup>2</sup> that the only “significant feature” is the one in the GC, while all the other features, found in 1205.4700v1 can be considered as pure statistical fluctuations.

We believe that the current data do not allow to reach a definitive conclusion here. Moreover, the most relevant question is actually different. To support the DM interpretation of the GC line, one should try to determine:

- Is it possible to *exclude* the existence of features in several regions around the Galactic plane (apart from the GC)?

We demonstrate in this work that the answer to this question is *negative* – the data does not allow to separate with confidence a feature in the Galactic Center from other features in the Galactic plane. Moreover, common interpretation of all the features is possible, providing additional evidence for such a hypothesis. Therefore, that the *nature of all these deviations* from simple featureless spectral models at energies 50–200 GeV should be discussed, rather than some peculiar properties of the Galactic Center region. Until this question is

\* Corresponding author. Tel.: +380 674198193.

E-mail address: [dmalyshev@bitp.kiev.ua](mailto:dmalyshev@bitp.kiev.ua) (D. Malyshev).

<sup>1</sup> The latter paper has appeared after the first version of the present work 1205.4700v1.

<sup>2</sup> See also talks by C. Weniger at IDM-2012 [19] and COSMO-2012 [20] conferences.

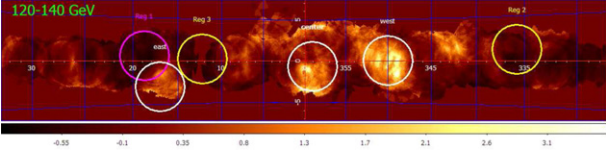


**Fig. 1.** Difference in the number of photons between the energy bin 120–140 GeV and the half-sum of two adjacent bins (100–120 and 140–160 GeV). The regions with positive and negative excesses around the background are clearly visible. Three most significant regions from [3] are shown with white circles.

settled the DM origin of the 130 GeV line (or a pair of lines at 110 and 130 GeV) remains dubious.

## 2. Identifying regions with spectral features in the Galactic planes

For the analysis presented below we used 209 weeks of Fermi data and v9r23p1 Fermi Software. We filter the photons with the expression `(DATA_QUAL==1) && (LAT_CONFIG==1) && (ABS(ROCK_ANGLE)<52) && ((STOP<352773002.0) || (START>352814402.0))` recommended by the Fermi-team in order to exclude a bright solar flare that affected Fermi on March 8, 2012.<sup>3</sup>

### 2.1. Residual maps

We start by searching for regions around the Galactic plane ( $|l| \leq 30^\circ$ ,  $|b| \leq 5^\circ$ ) which have excesses at different energies. To this end we split the energy range 80–200 GeV into six energy bins, 20 GeV each (at energies of interest the spectral resolution of Fermi is about 10%). In each energy bin we build a count maps using CLEAN class of photons and smooth each map with a tophat filter with the radius of  $3^\circ$ , obtaining images  $I_i$ ,  $i = 1, \dots, 6$ . For each image  $I_i$  we then define a “background” as  $B_i = \frac{1}{2}(I_{i-1} + I_{i+1})$ . In order to identify regions with spectral features we built then a set of images  $A_i = I_i/B_i - 1$ . Such a map for 120–140 GeV energy band is shown in Fig. 1. The positive (negative) color coding at these images corresponds to the regions with positive (negative) excess in the spectrum. Three regions with the most significant excess from [3] are marked on the map as white circles. The positions of white circles obviously correspond to the positions of (some of) the brightest excesses on this map. It is clearly seen in Fig. 1 that emission around the GC region is shifted from  $(l, b) = (0, 0)$ .

Notice, however, that excesses of similar significance are visible not only on 120–140 GeV map (Fig. 1), but also on the maps 100–120 GeV and 140–160 GeV (Fig. 2). We identified three additional regions that show high signal/background ratio: REG 1 and REG 2 regions are bright on 100–120 GeV map, while REG 3 region is bright on 140–160 GeV. All these regions are circles with  $3^\circ$  radius, as are the regions of [3].<sup>4</sup>

The resulting spectra in the energy range 50–200 GeV extracted from the regions REG 1, REG 2, and REG 3 together with the CENTRAL region (coinciding with the region of the most significant excess of [3] around the GC) are shown in Fig. 3. The spectra from all the regions REG 1, REG 2, and REG 3 clearly show a number of features at different

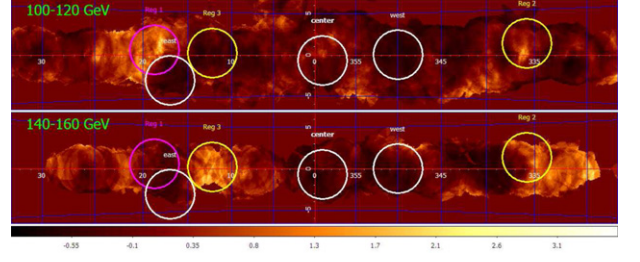


**Fig. 2.** Same as in Fig. 1 but showing the difference of 100–120 GeV and 140–160 GeV energy bins with the half-sum of two corresponding adjacent bins. Yellow and magenta circles mark bright excesses on these maps, see text for the details. The radii of all circles are  $3^\circ$ . (For interpretation of reference to color in this figure legend, the reader is referred to the web version of this article.)

energies. The thickness of the lines representing the spectra in Fig. 3 is defined by the formal  $1\sigma$  statistical error.

### 2.2. Analysis of the spectral features

In order to quantify the significance of the observed spectral features in the regions REG 1, REG 2, REG 3 we start with performing a power law fit

$$N(E) = N_{100}(E/100 \text{ GeV})^{-\Gamma}, \quad (1)$$

to the data. The reduced  $\chi^2$  and the resulting  $p$ -values are presented in Table 1, columns (a–d). Here the  $p$ -values are defined as

$$p\text{-value} = \int_{\chi_0^2}^{\infty} P_n(\chi^2) d\chi^2, \quad (2)$$

where  $P_n(\chi^2)$  is the probability density function of the  $\chi^2$  distribution with  $n$  degrees of freedom.

Looking at the quality of fit to the power law model in 50–200 GeV energy range one could have concluded that with 20–40% probability the data is consistent with *being described purely by the power law without any features* (even in the CENTRAL region this probability is more than 3%). Based on a similar analysis, it was argued (see e.g. [19,20]) that the features in the regions REG 1, REG 2, REG 3 are not statistically significant.

However, as was discussed in Section 1, the relevant question is whether one can demonstrate with confidence that the line is *not* present in the spectrum of the regions REG 1–REG 3 and that the observed photon counts are simply statistical fluctuations around a featureless model. Below we argue that this is not the case.

We notice first of all, that the quality of fit (and therefore the conclusion about “chance probability” of a given  $\chi^2$ ) is sensitive to the inclusion or omission of the bins with  $E \geq 150$  GeV (as comparison of the columns (a) and (b) in Table 1 demonstrates). These bins have extremely low statistics (0–2 counts) and their large error bars artificially improve the fit quality (as the comparison of the columns for  $\chi_{20-150}^2$  and  $\chi_{50-200}^2$  demonstrates). Inclusion of even larger number of empty bins with  $E > 200$  GeV would further improve the quality of fit. At the same time, the change of the interval can change the resulting  $p$ -values by as much as the order of magnitude (see the columns (c) and (d) in Table 1).

A way to determine whether a spectral feature is a fluctuation (that is at least partially free from the above-described ambiguities) is to add an additional component (Gaussian or other spectrally localized feature) and see whether the quality of fit improves. In doing this, we see that for REG 1, REG 3 and CENTRAL regions the quality of fit improves (by 2– $3\sigma$ ). The results are presented in Table 3.

This method, however, crucially depends on our knowledge of a spectral shape of a feature. As a result, we cannot characterize in this way, for example, the region REG 2, where the feature at 70–100 GeV

<sup>3</sup> The large area telescope (LAT) on board the Fermi satellite is a pair-conversion gamma-ray detector operating between 20 MeV and 300 GeV. The LAT has a wide field of view of  $\sim 2.4$  sr at 1 GeV, and observes the entire sky every two orbits ( $\sim 3$  h for a Fermi orbit at an altitude of  $\sim 565$  km, full details of the instruments are given in [21]).

<sup>4</sup> Any difference between the “residual maps” between CLEAN and ULTRACLEAN events would signify that these residuals are parts of some known systematics (e.g. contamination from cosmic rays) [4]. We have verified that one obtains the same maps when using ULTRACLEAN photon class.

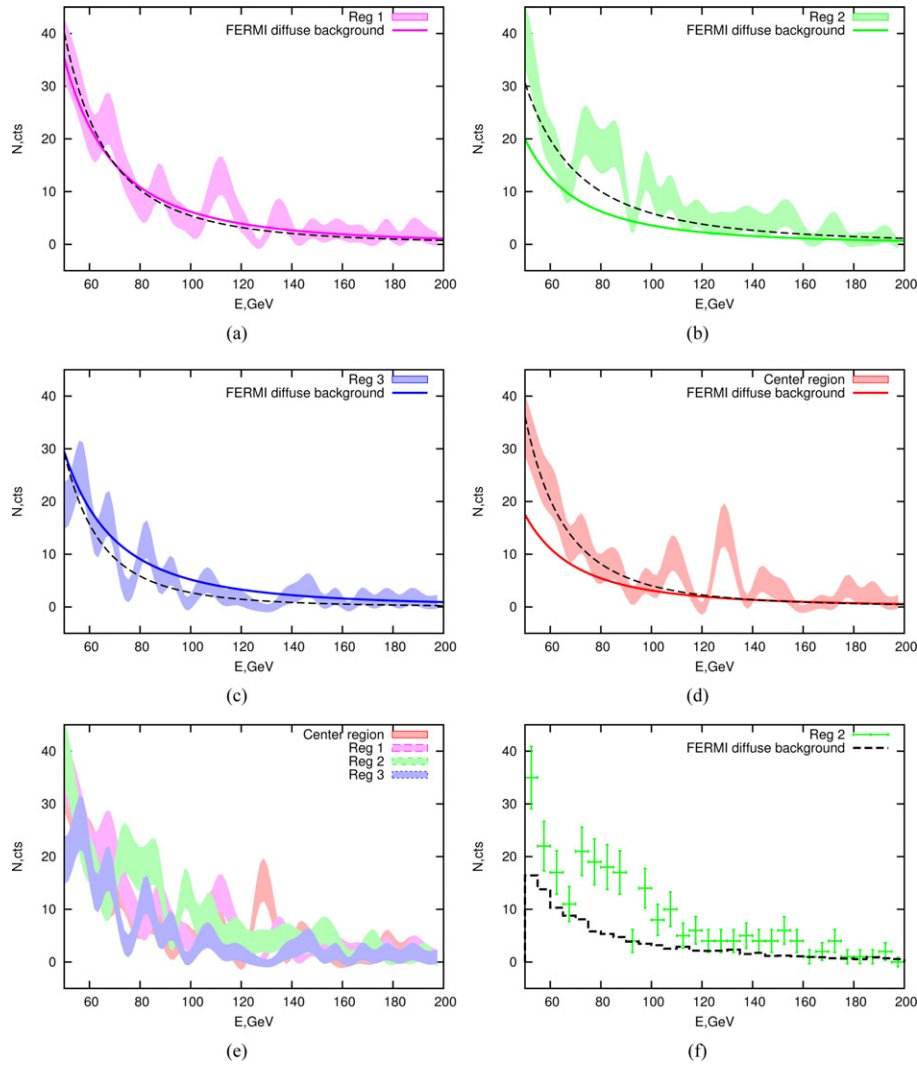


**Fig. 3.** Spectra from the REG 1 region (magenta line), panel (a), REG 2 (panel (b)), REG 3 (panel (c)) and CENTRAL region (panel (d)). The definitions of the regions are shown in Fig. 2. The best fit power law for the spectrum is shown in black dashed line (panels (a)–(d)), the best fit diffuse FERMI background model is shown with solid color line. The thickness of the spectra is determined as  $\pm 1\sigma$  around the central value. All spectra together are shown in panel (e). The spectrum of REG 2 with 10 GeV energy binning together with the corresponding prediction from the FERMI diffuse background model is given in panel (f) for comparison (see Section 2.3 for details). (For interpretation of reference to color in this figure legend, the reader is referred to the web version of this article.)

**Table 1**  
The values of  $\chi^2/\text{d.o.f.}$  when fitting the power law model (1) to the data in the energy range 50–200 GeV (column (a)) and 20–150 GeV energy range (column (b)). Columns (c) and (d) show the chance probability  $p$  to get observed  $\chi^2$  values (as defined by Eq. (2)). The significances that correspond to these  $p$ -values are given in columns  $S_{50-200}$  and  $S_{20-150}$ . The change of the fitting interval may affect the  $p$ -values by as much as an order of magnitude.

Region	$\chi^2_{50-200}/28$ (a)	$\chi^2_{20-150}/24$ (b)	$p_{50-200}$ (c)	$p_{20-150}$ (d)	$S_{50-200} [\sigma]$ (e)	$S_{20-150} [\sigma]$ (f)
REG 1	1.19	1.64	0.224	$2.5 \times 10^{-2}$	1.22	2.24
REG 2 (shifted)	1.21	1.35	0.205	0.117	1.27	1.57
REG 3	1.05	1.49	0.392	$5.8 \times 10^{-2}$	0.86	1.90
GC	1.53	1.78	$3.6 \times 10^{-2}$	$1.1 \times 10^{-2}$	2.10	2.54

**Table 2**  
The most significant features in the regions REG 1, REG 2, REG 3, and CENTRAL. We fit the background counts to the power law model in the whole 50–200 GeV energy range (unless otherwise specified) and determine the most prominent deviations from this simple background model and their significance (column (e)). This significance of the spectral feature is defined as the Poisson probability to observe  $N$  counts or more, provided that the spectral model predicts  $\lambda$  counts (specified in the column (d)).<sup>a</sup>

Region ( $l^\circ, b^\circ$ ) (a)	Prominent features, energy range (b) (GeV)	Observed counts (c)	Predicted by model (d)	Significance of spectral feature (e)
REG 1 ( $18.72^\circ, 0.57^\circ$ )	105–120	29	10.46	4.63
REG 2 ( $335.76^\circ, 1.255^\circ$ )	70–90	75	40.95	4.72
REG 2 ( $335.76^\circ, 1.255^\circ$ )	95–110	32	16.83	3.23
REG 3 ( $12.22^\circ, 0.20^\circ$ )	80–85	13	5.25	2.74
CENTRAL ( $359^\circ, -0.7^\circ$ )	125–135	25	3.53	7.34
	105–115	17	5.99	3.58

<sup>a</sup> This definition of significance is different from the one, used in [2]. See the discussion in Section 3.

**Table 3**

Change in the total  $\chi^2$  when adding a Gaussian at 130 GeV (CENTRAL), at 112.5 GeV (REG 1) and at 85 GeV (REG 3) as compared to the power law fits, shown in Table 1. A formal significance of these features is defined as  $\sqrt{\Delta\chi^2}$  (as we add only one degree of freedom when fitting a normalization of the Gaussian). The features in the region REG 2 do not have a Gaussian shape and we do not show it in this table.

Region	$\chi^2_{20-150}/23$ power law + Gaussian fit	$\Delta\chi^2$	Significance of a feature [ $\sigma$ ]
CENTRAL	1.179	15.6	3.95
REG 1	1.339	8.6	2.93
REG 3	1.375	4.1	2.02

is clearly non-Gaussian. Therefore we also compute the local significance of these features — the Poisson probability to observed  $n$  counts or more in a given bin, provided that the model predicts  $\lambda$  counts. The results are presented in Table 2 and in Fig. 4. Clearly, such a *local significance* should be higher than the  $p$ -value, presented in Table 1. And indeed, in the spectrum of the CENTRAL region we recover an excess at 130 GeV at  $7.34\sigma$  and a  $3.6\sigma$  excess in the energy bin around 110 GeV line. The spectrum of the REG 1 region demonstrates an excess above the power law fit at energy  $\sim 115$  GeV with the significance  $4.63\sigma$  (Fig. 3a). The spectrum of the REG 2 region (Fig. 3b) formally has a reasonable power law fit in the range 60–200 GeV (reduced  $\chi^2 = 1.19$  for 28 degrees of freedom). However, the distribution of residuals in this region shows a broad positive fluctuations in the range 70–120 GeV. Indeed, a power law fit to the subset of the data (energies 60–110 GeV) is extremely poor (the reduced  $\chi^2 > 2$ ). However, in the region 110–200 GeV the data points have just few counts and therefore large statistical errors reduce the overall  $\chi^2$  value to acceptable values close to 1. Finally, in the region REG 3 we observed a line-like feature at 80 GeV (and a possible additional feature around 140–150 GeV) with significance around  $3\sigma$ . Notice that positions of both features in REG 3 coincide with the peaks in the local significance of the REG 2. We also checked that thus determined significance does not depend on the number of bins (the maxima of the lines of different color in the panels of Fig. 4 coincide). Notice, that the bin of 20 GeV is much wider than the spectral resolution of the Fermi satellite at these energies (about 10 GeV), suggesting that this is *not* a line-like feature (whose width should be 10% of the energy) but rather a power law with a sharp cut-off (as e.g. in [15]).

In order to further clarify the significance of the observed features (and correct for possible “trial factors”), we perform  $10^4$  Monte Carlo realization of the background (power law) model for regions REG 1, REG 2 and CENTRAL (see Fig. 5). In all panels 99.9% of all realizations are inside the dashed lines. Feature at 130 GeV in the CENTRAL region (Fig. 5a) lies clearly outside these lines, which means that the significance of the feature is *above*  $3\sigma$ . Feature at 110 GeV in REG 1 (Fig. 5b) is also a  $3\sigma$  deviation.<sup>5</sup> Notice, that in case of the REG 2 our simulations provide a conservative estimate of significance. The described procedure does not take into account that in the spectrum of this region *several consecutive bins* deviate from the power law model. This analysis allows us to conclude that, although the spectral feature at the GC is more significant (possibly due to the lower *predicted* background at 130 GeV as compared to lower energies), *the presence of the spectral features in other regions cannot be ruled out with confidence*.<sup>6</sup>

<sup>5</sup> The discrepancy between the  $p$ -value, deduced from Monte Carlo simulations, and  $p$ -values, listed in Table 1, is of course not surprising –  $\chi^2$  is a global measure of the quality of fit, while the features that we are discussing are localized to several consecutive bins.

<sup>6</sup> The regions REG 1, REG 2, REG 3, discussed so far, as well as the regions where the most significant excess is observed in [3], are located in the different regions along the Galactic plane. In [2], however, the excess at 130 GeV was claimed to originate from a large region, mostly located outside the Galactic plane (its approximate shape is shown in Fig. 9, left panel). Removing the central box of  $3^\circ \times 3^\circ$  (about 10% of the total field of

**Table 4**

Change of the *test statistics* (TS) when fitting spectral and spatial distribution of photons to a smooth background model and to the same model with an additional line (see Section 2) The line has Gaussian spatial profile with  $3^\circ$  FWHM and Gaussian spectral profile with 5 GeV dispersion on top of Fermi diffuse background models. The TS maps are shown in Fig. 6. The  $TS_{\max}$  column shows the maximum difference of likelihoods over all pixels within a given region.

Region ( $l^\circ, b^\circ$ )	Energy of the line (GeV)	$TS_{\max}$
REG 1 (18.72°, 0.57°)	110	14.99
REG 2 (335.76°, 1.255°)	80	32.3
	110	17.26
REG 3 (12.22°, 0.20°)	80	2.74
CENTRAL (359°, −0.7°)	130	21.22
	110	4.5

### 2.3. Test statistics maps based on Fermi diffuse background model

One possible interpretation of the above results is that by exploring regions outside the GC one increases the “trial factors” by  $10^\circ \times 60^\circ / (\pi \times 3^\circ \times 3^\circ) \approx 21$  (and therefore  $p$ -values of the features, obtained above, should be further penalized by this factor). This would be the case if spectra in all  $3^\circ$  circles around the Galactic plane were completely arbitrary, not correlated with each other. This is however, not true in our case, as the diffuse emission in the Galactic plane is described by the smooth model.

To study both spectral and spatial variations of emission around the Galactic plane, we model  $50^\circ \times 50^\circ$  region (in J2000 coordinates) around the GC by three components — standard galactic (centered at GC) and extragalactic Fermi backgrounds<sup>7</sup> and a model of a “line”, that we try to add in each pixel in order to improve the fit (pixel size is  $0.5^\circ \times 0.5^\circ$ ). The “line” model has Gaussian spatial profile with  $3^\circ$  FWHM and Gaussian spectral profile with 5 GeV dispersion, centered correspondingly at 80 GeV, 110 GeV, 130 GeV.<sup>8</sup> We fit the data with the diffuse models and then consider the change of the log-likelihoods of the fit when adding the Gaussian component at these three energies. We build the map of TS values (the difference of log-likelihoods of two models) using `gttsmap` tool. The normalizations of the Fermi diffuse backgrounds, as well the normalization of the region model were allowed to vary during the fit procedure. The test-statistics values of the  $3^\circ$ -region model fits are shown in Fig. 6. The significance of the model can be estimated as  $\sqrt{TS}\sigma$ .

The test-statistical value of the line centered at CENTRAL region is about 21, that corresponds to significance  $\sim 4.5\sigma$ . Beside the CENTRAL region Fig. 6 exhibit additional regions with the excesses at 70–90 GeV (Fig. 6c) and 100–120 GeV (Fig. 6b). Notice that, contrary to the results of [4], the test statistics of the CENTRAL region does not improve significantly when adding a Gaussian at 110 GeV, i.e. photon distribution in this energy bin strongly deviates from  $3^\circ$  FWHM spatial Gaussian profile. The highest test statistics  $TS = 32.3$  is found in the region REG 2 at 80 GeV (see Table 3 for details).

### 3. Discussion and conclusions

The first version of this paper (1205.4700v1) demonstrated that spectra of several regions (e.g. REG 1, REG 2, REG 3) are not featureless at energies  $E > 50$  GeV, but contain excesses similar in significance

view) we see that the significance of the feature at 130 GeV drops (green vs. blue data points in the right panel in Fig. 9). Therefore, we conclude that the feature at 130 GeV is related to the region close to the Galactic Center, without inclusion of this region the feature becomes insignificant (a similar conclusion was reached in [3,4]).

<sup>7</sup> Given by `gal_2yearp7v6_v0.fits` and `iso_p7v6clean.txt` templates, see e.g. <http://fermi.gsfc.nasa.gov/ssc/data/access/lat/BackgroundModels.html>.

<sup>8</sup> We have repeated the same exercise with the Gaussian line, having 2 GeV FWHM and obtained similar results.



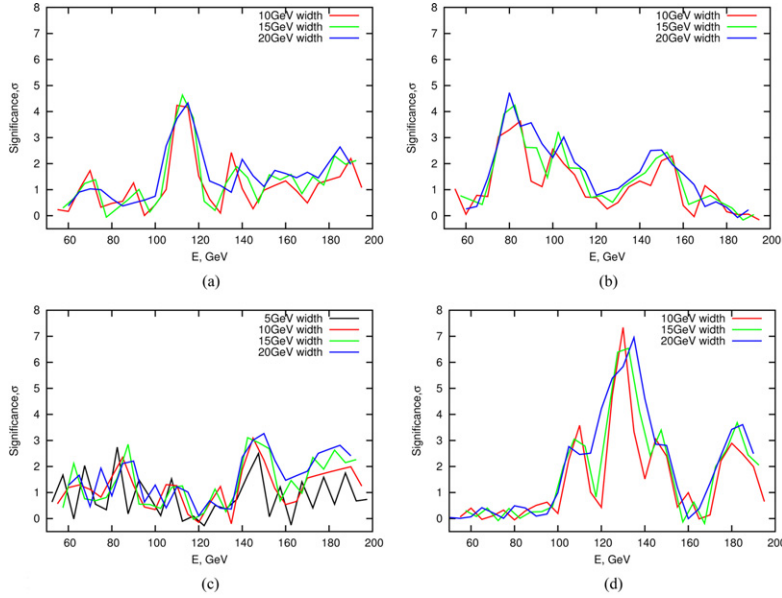


**Fig. 4.** Local significance of observing fluctuations in 2, 3 and 4 consecutive bins (with 10, 15 and 20 GeV width correspondingly), as a function of energy. The significance is defined as the Poisson probability to observe  $N$  or more counts, when the model predicts  $\lambda$  (based on the power law background model). Notice that the significance does not depend on the number of consecutive bins that we choose! (a) REG 1. A feature at 110 GeV is clearly visible, (b) REG 2. A broad feature in the region 70–100 GeV is clearly visible, (c) REG 3. Possible features are around 80 GeV and around 150 GeV (compare excess in REG 2 region at these energies). Notice that for this region we also added one bin local significance. (d) CENTRAL. A strong feature around 130 GeV and a possible second feature around 110 GeV.

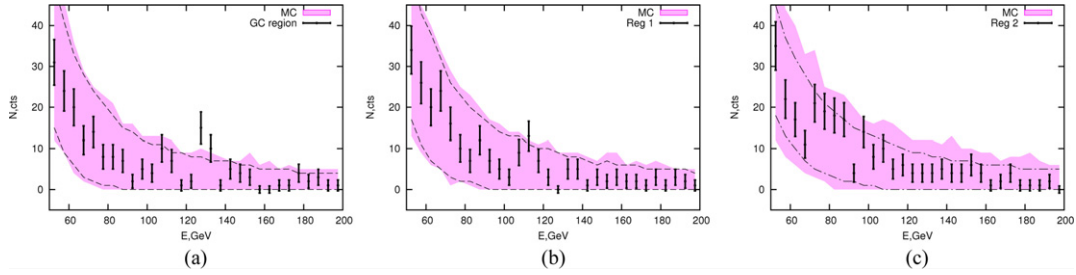


**Fig. 5.** Monte Carlo realizations of the power law models in the region 50–200 GeV for CENTRAL (left), REG 1 (center) and REG 2 (right) regions. Number of realization is  $10^4$ . Shaded regions show minimum and maximum number of counts in all the Monte Carlo realizations. 99.9% of all realizations lie between dashed lines (in panel (c) dashed-dotted line show 99% of all models). Data points outside dashed lines are at least  $3\sigma$  deviations from the power law model. Two data points in the panel (c) deviate from the power law by  $2.3\sigma$ . (a) Region CENTRAL. Result of  $10^4$  Monte Carlo realizations, of which 99.9% lie between dashed lines. Significance of the feature at 130 GeV is more than  $3\sigma$ . (b) Region REG 1. Result of  $10^4$  Monte Carlo realizations, of which 99.9% lie between dashed lines. Significance of the feature at 110 GeV is more than  $3\sigma$ . (c) Region REG 2. Result of  $10^4$  Monte Carlo realizations, of which 99% lie between dashed-dotted lines. Significance of each deviation is above  $2.3\sigma$ .

to the spectral feature in the GC region. In particular, version 1 found excess in 110 GeV bin from the REG 1 (a pair of lines at  $\sim 110$  and  $\sim 130$  GeV from the GC region was later discussed in [4]). Our present analysis recovers the previous results with high significance and our main conclusion remains intact – with the current data it is impossible to rule out the possibility that the observed spectral features are actual signals (of astrophysical or instrumental origin), rather than statistical fluctuations of the smooth backgrounds. Clearly, until such a possibility is ruled out, the DM interpretation of the emission from the GC remains dubious.

Refs. [4,18] also analyzed *spatial* distribution of residuals and significance of different regions around the Galactic plane. The analysis, presented here, and the interpretation of the significance of the spectral features is different due to the different statistical approaches adopted.

One way to detect spacial “hot spots” with significant spectral features is just to look for the regions where the best fit to a smooth (power law) model is unacceptable (i.e. the reduced  $\chi^2 \gg 1$ ). This method was discussed e.g. in [19,20]. The results of such fits for our regions were presented in Table 1. This method however, is prone to a number of uncertainties, related to the choice of fitting interval and

to the fact that  $\chi^2$  is a global measure of fit, where the significance of local spectral features can be “blurred” by many bins with large errors bars. Indeed, as demonstrated in Section 2.2 the *local significance* of the features, found in regions REG 1, REG 2, and REG 3 is higher than predicted by this method ( $3\sigma$  and above).

A common way to determine the significance of these hot spots is to multiply the resulting  $p$ -values of the spectral features by the number of regions that were used in the search for the “hot spots” (so called “trial factors”, see e.g. [4]). The number of regions is, however, totally subjective and the resulting significance can be artificially lowered (or increased). We believe that a better way to account for spatial distribution of residuals is to find a smooth background model that fits the data in (most of the) spatial regions and deviation from which are normally distributed (modulo some localized spots) (a similar approach was used in [4]). We used the galactic diffuse background by the Fermi collaboration as such a spatial model. We see (Fig. 6) that this model correctly fits the data “almost everywhere” apart from several localized spots where it underpredicts the number of photons and where additional Gaussian strongly improves the quality of fit. The histogram (Fig. 7) clearly shows that the distribution of pixels with  $TS \lesssim 8$  is consistent with the  $\chi^2$  distribution with 1 degree of

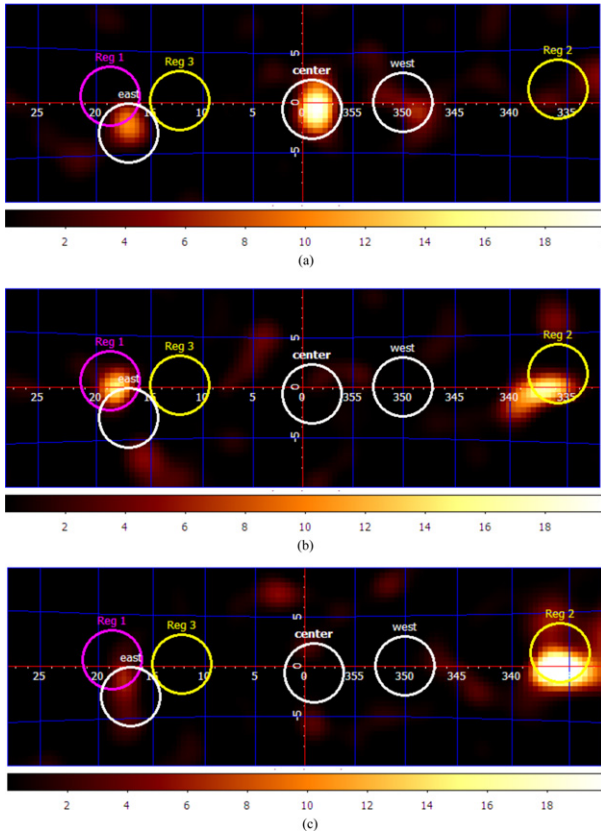


**Fig. 6.** Test-statistics (TS) maps when in addition to Galactic and extragalactic Fermi backgrounds we add a model of the  $3^\circ$ -region centered at this point. The latter was taken to have Gaussian spatial profile with  $3^\circ$  FWHM and Gaussian spectral profile with 5 GeV dispersion, centered correspondingly at 80, 110, 130 GeV. (a) Energy range 120–140 GeV. The maximal TS  $\approx 21.2$  is located at the pixel with  $(l, b) \approx (-1.5^\circ, -0.75^\circ)$ . (b) Energy range 100–120 GeV. The maximal TS in REG 1 is TS  $\approx 15.0$  is located at the pixel with  $(l, b) \approx (18.1, 0.2)$  and in the region REG 2 the maximal TS is  $\approx 17.3$ , located at the position  $(l, b) = (337.1, -0.2)$ . (c) Energy range 70–90 GeV. The maximal TS  $\approx 32.3$  is located at the pixel with  $(l, b) \approx (336.0, -0.2)$ .

freedom (as it should be for statistical fluctuations). However, there are also few *high* TS outliers, corresponding to the hot spots in Fig. 6a–c).<sup>9</sup> These regions are the GC and several other regions (REG 1 and REG 2) that we have previously identified in Figs. 1 and 2.

Looking at Fig. 3, one notices that in these regions Fermi model systematically (in many consecutive bins) underpredicts the data (this is also true for the GC region).<sup>10</sup> As Fermi diffuse model is determined globally, one cannot improve the quality of fit in these spots without worsening the overall fit. In all these regions the signal is consistent with the smooth background model plus additional sources of emission with sharp energy spectra localized in the Galactic plane.

Indeed, let us compare two most prominent regions (CENTRAL and REG 2) (Fig. 3b and d). We can interpret their spectra as a combination of spatially smooth (Fermi) background model plus a localized excess modeled in each region by two components: a low-energy (20–80 GeV) power law and a feature at energies around  $\sim 70$ –80 GeV for REG 2 and 110–130 GeV for CENTRAL regions. The count rates observed in these features (number of counts in excess of the background model) are approximately the same, the significance of the feature is thus determined only by the *predicted background value*. This value of the

<sup>9</sup> There are about 133 independent  $3^\circ \times 3^\circ$  pixels in the region  $(|l| \leq 30^\circ, |b| \leq 10^\circ)$  that we used for this analysis. If all positive TS are caused just by statistical fluctuations, one expects (roughly) one outlier with TS  $\approx 9$  for  $\sim 300$  pixels.

<sup>10</sup> If one excludes from fit several outlier bins, the resulting power law model becomes much closer to the predictions of Fermi background.

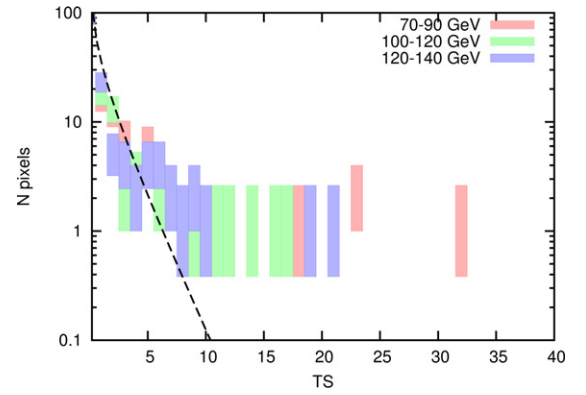


**Fig. 7.** Distribution of test statistics (TS) when adding a fixed width (in space and in energy) Gaussian in different positions in the Galactic plane (as described in Section 2, see also Fig. 6a–c). Dashed line is the  $\chi^2$  distribution with 1 degree of freedom. If all pixels with TS  $> 0$  in Fig. 6 are merely statistical fluctuations, one should see that the number of pixels for each TS is consistent with the dashed line and as a result there are no pixels with TS  $\gtrsim 8$  (for the number of pixels that we have in our regions). However, if high-TS outliers for CENTRAL, REG 2, REG 1, etc. are not caused by statistical fluctuations only, one should see a tail of large TS (as indeed seen in this Figure).

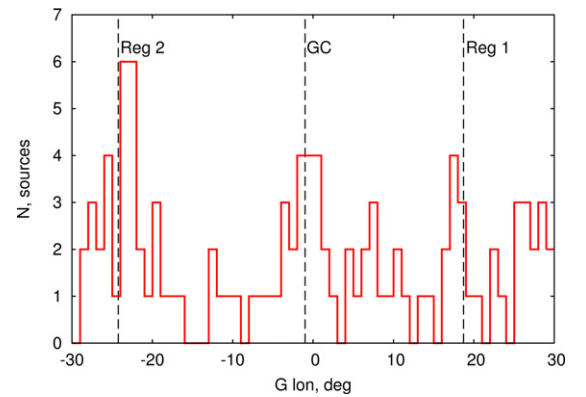


**Fig. 8.** Number of 2FGL sources at different positions along the Galactic plane ( $|b| \leq 3^\circ$ ). Positions of regions CENTRAL, REG 2 and REG 1 are clearly visible as local maxima in the number of sources.

predicted signal decreases with energy, therefore the most energetic (130 GeV) feature, having the count rate close to that of features at other energies, would have a higher significance against very low background at that high energy.

An additional evidence in favor of the “local source” hypothesis is provided by the histogram of the number of point sources from the 2 year Fermi catalog along the Galactic plane (shown in Fig. 8). One sees that the regions CENTRAL, REG 2 and REG 1 correspond to the local maxima in the concentration of point sources in the Galactic plane. This picture is consistent with having some additional localized sources of emission in some regions along the Galactic plane.

*In conclusion*, at the moment there are two possible interpretations of the observed features. In one of them the 130 GeV feature is assumed to be a unique statistically significant feature (probably explained by DM annihilation/decay) see e.g. [2,3], while all other features are treated as fluctuations of the powerlaw background. The other possible interpretation is that all the features at 80 GeV, 110 GeV, 130 GeV observed in the spectra of different parts of the Galactic plane have a similar origin. Our analysis shows that the present data is consistent with “many features – many sources” interpretation. If confirmed, such interpretation would be hard to explain in terms of Dark Matter annihilation (or decay), it would probably require an astrophysical explanation, like, for example the one of [15], in which narrow spectral features (located at different energies for different systems) are produced by emission from ultra-relativistic

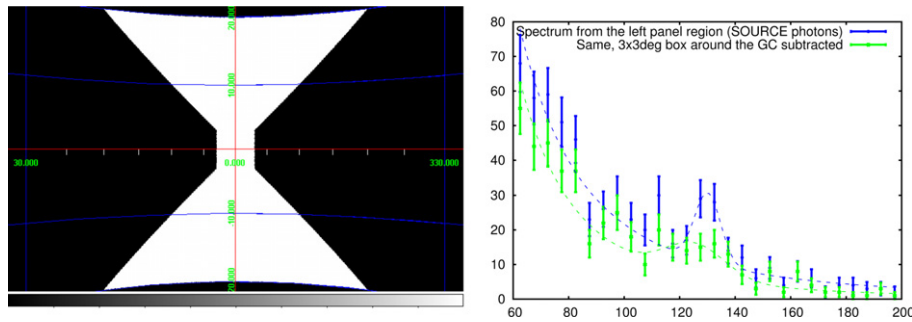


**Fig. 9.** *Left panel:* region that approximately coincides with the “Region 3” of [2] and reproduces its spectrum. *Right panel:* Spectrum of this region (blue) with the feature at 130 GeV clearly visible. The same spectrum extracted from the region with removed central  $3^\circ \times 3^\circ$  box (green) and decreased significance of 130 GeV feature. (For interpretation of reference to color in this figure legend, the reader is referred to the web version of this article.)

pulsar wind.

If this interpretation will be confirmed by the future data, this means that a line-like feature in  $\gamma$ -ray spectrum should not necessarily be “a smoking gun” of dark matter annihilation (or decay), as it is often assumed. In Refs. [2,4,18] a procedure of data analysis is described in which only the most significant (located in the GC) feature survives while all other regions have their significances below  $3\sigma$ . However, to speak seriously about the DM origin of a signal, one has to show that no other interpretation is possible (for example, that the other features may *not* have physical origin). We believe that for the moment the data does not allow to distinguish reliably between these two interpretations. Additional observations with HESS-2, Gamma-400 and CTA will probably be required in order to check these models (see [22]), but until that the DM interpretation of 130 GeV feature and treating all other features in a different way looks dubious.

## Acknowledgments

We acknowledge useful discussions with G. Bertone, C. Frenk, G. Servant, M. Su. We are especially thankful to D. Finkbeiner and C. Weniger for fruitful discussions, comments on our manuscript and for sharing with us their results prior to publication. O.R. would like to thank the organizers of the IDM 2012 conference for setting up a special discussion session. The work of D.M. is supported in part from the SCOPES project IZ73Z0.128040 of Swiss National Science Foundation, Grant no. CM-203-2012 for young scientists of National Academy of Sciences of Ukraine, Cosmomicphysics programme of the National Academy of Sciences of Ukraine and by the State Programme of Implementation of Grid Technology in Ukraine. D.M. thank the participants of ISSI team “Present and Past Activity of the Galactic Center Super-massive Black Hole” for useful discussions and the International Space Science Institute (ISSI, Bern) for support. The authors also wish to acknowledge the SFI/HEA Irish Centre for High-End Computing (ICHEC) for the provision of computational facilities and support.

## References

- [1] T. Bringmann, X. Huang, A. Ibarra, S. Vogl, C. Weniger, Fermi LAT search for internal bremsstrahlung signatures from dark matter annihilation, ArXiv e-prints (2012), arXiv:1203.1312.
- [2] C. Weniger, A tentative gamma-ray line from dark matter annihilation at the Fermi large area telescope, ArXiv e-prints (2012), arXiv:1204.2797.
- [3] E. Tempel, A. Hektor, M. Raidal, Fermi 130 GeV gamma-ray excess and dark matter annihilation in sub-haloes and in the Galactic centre, ArXiv e-prints (2012), arXiv:1205.1045.
- [4] M. Su, D.P. Finkbeiner, Strong evidence for gamma-ray line emission from the inner galaxy, ArXiv e-prints (2012), arXiv:1206.1616.
- [5] L. Bergstrom, H. Snellman, Observable monochromatic photons from cosmic photino annihilation, Phys. Rev. D37 (1988) 3737–3741.
- [6] L. Bergstrom, Dark matter evidence, particle physics candidates and detection methods, arXiv:1205.4882.
- [7] T. Bringmann, C. Weniger, Gamma ray signals from dark matter: concepts, status and prospects, arXiv:1208.5481.
- [8] C. Jackson, G. Servant, G. Shaughnessy, T.M. Tait, M. Taoso, Higgs in space!, JCAP 1004 (2010) 004, arXiv:0912.0004.
- [9] ATLAS Collaboration. G. Aad, et al. Observation of a new particle in the search for the Standard Model Higgs boson with the ATLAS detector at the LHC, Phys. Lett. B (2012), arXiv:1207.7214.
- [10] CMS Collaboration. S. Chatrchyan, et al. Combined results of searches for the standard model Higgs boson in pp collisions at  $\sqrt{s} = 7$  TeV, Phys. Lett. B710 (2012) 26–48, arXiv:1202.1488.
- [11] S. Profumo, T. Linden, Gamma-ray Lines in the Fermi data: is it a Bubble? arXiv:1204.6047.
- [12] E. Dudas, Y. Mambrini, S. Pokorski, A. Romagnoni, Extra U(1) as natural source of a monochromatic gamma ray line, arXiv:1205.1520.
- [13] A. Ibarra, S. Lopez Gehler, M. Pato, Dark matter constraints from box-shaped gamma-ray features, arXiv:1205.0007.
- [14] J.M. Cline, 130 GeV dark matter and the Fermi gamma-ray line, 1205.2688 (4 pages, 5 figures).
- [15] F. Aharonian, D. Khangulyan, D. Malyshev, Cold ultrarelativistic pulsar winds as potential sources of galactic gamma-ray lines above 100 GeV, arXiv:1207.0458.
- [16] LAT Collaboration. M. Ackermann, et al., Fermi LAT search for dark matter in gamma-ray lines and the inclusive photon spectrum, arXiv:1205.2739.
- [17] A. Hektor, M. Raidal, E. Tempel, Fermi-LAT gamma-ray signal from Earth Limb, systematic detector effects and their implications for the 130 GeV gamma-ray excess, arXiv:1209.4548.
- [18] D.P. Finkbeiner, M. Su, C. Weniger, Is the 130 GeV line real? A search for systematics in the Fermi-LAT data, arXiv:1209.4562.
- [19] C. Weniger, Talk at IDM-2012. <<http://kicp-workshops.uchicago.edu/IDM2012/depot/talk-weniger-christoph.pdf>>, 2012.
- [20] C. Weniger, Talk at COSMO-2012. <<http://lss.bao.ac.cn/cosmo12/talk/0910dm/COSMO12.dm0910p.ChristophWeniger.pdf>>, 2012.
- [21] W.B. Atwood, et al. The large area telescope on the Fermi gamma-ray space telescope mission, Astrophys. J. 697 (2009) 1071–1102, arXiv:0902.1089.
- [22] L. Bergstrom, G. Bertone, J. Conrad, C. Farnier, C. Weniger, Investigating gamma-ray lines from dark matter with future observatories, arXiv:1207.6773.